

***BeppoSAX* Observation of NGC 7582: Constraints on the X-ray absorber**

T.J.Turner ^{1,2}, G.C. Perola, ³, F. Fiore, ^{4,5}, G. Matt, ³, I.M. George ^{1,6}, L. Piro, ⁷, L. Bassani ⁸

ABSTRACT

This paper presents a *BeppoSAX* observation of NGC 7582 made during 1998 November and an optical spectrum taken in 1998 October. The new X-ray data reveal a previously unknown hard X-ray component in NGC 7582, peaking close to 20 keV. Rapid variability is observed with correlated changes in the 5-10 and 13-60 keV bands indicating that a single continuum component, produced by the active nucleus, provides the dominant flux across both bands. Comparison between *RXTE* and *BeppoSAX* data reveals changes in the 2 – 10 keV flux on timescales of months. Changes in the nuclear X-ray flux appear unrelated to the gradual decline in optical flux noted since the high-state in 1998 July. The 0.5 – 2 keV flux of NGC 7582 is not significantly variable within the *BeppoSAX* observation, but has brightened by a factor of ~ 2 since the *ASCA* observation of 1994. While there is some concern about contamination from spatially-unresolved sources, the long-term variability in soft X-ray flux seems most likely associated with the nucleus or an event within the host galaxy of NGC 7582.

The 2 – 100 keV spectrum is well fit by a powerlaw of photon index $\Gamma = 1.95^{+0.09}_{-0.18}$, steeper by $\Delta\Gamma \simeq 0.40$ than the index during the 1994 *ASCA* observation. The X-ray continuum is attenuated by a thick absorber of

¹LHEA, Code 660, NASA/Goddard Space Flight Center, Greenbelt, MD 20771

²University of Maryland Baltimore County, 1000 Hilltop Circle, Baltimore, MD 21250

³Dipartimento di Fisica, E. Amaldi, Universita degli Studi Roma Tre, Via della Vasca Navale 84, I-00146 Roma, Italy

⁴SAX/SDC Nuova Telespazio, Via Corcolle 19, I-00131 Roma, Italy

⁵Osservatorio Astronomico di Roma, Via dell'Osservatorio, I-00044 Monteporzio-Catone, Italy

⁶Universities Space Research Association

⁷Istituto Tecnologie e Studio Radiazioni Extraterrestri, CNR, Via Gobetti 101, I-40129 Bologna, Italy

⁸Istituto di Astrofisica Spaziale, CNR, Via Fosso del Cavaliere, I-00133 Roma, Italy

$N_H \sim 1.6 \times 10^{24} \text{cm}^{-2}$ covering $\sim 60_{-14}^{+100}\%$ of the nucleus plus a screen with $N_H \sim 1.4 \times 10^{23} \text{cm}^{-2}$ covering the entire nucleus. Comparison of the *BeppoSAX* and *ASCA* spectra shows an increase in the full screen by $\Delta N_H \simeq 7 \times 10^{22} \text{cm}^{-2}$ since 1994, confirming the absorption variability found by Xue et al. The increase in soft X-ray flux between 1994 and 1998 is consistent with the appearance of holes in the full screen allowing $\lesssim 1\%$ of the nuclear flux to escape, and producing some clear lines-of-sight to the broad-line-region. The data are also consistent with the scenario suggested by Aretxaga et al, of the radiative onset of a type IIIn supernova causing the observed optical change in NGC 7582.

Subject headings: galaxies:active – galaxies:nuclei – galaxies:individual (NGC 7582) – X-rays: galaxies

1. Introduction

NGC 7582 ($z=0.0053$) is known as a Seyfert 2 galaxy and also as a Narrow Emission Line Galaxy (NELG). The former classification is made since the optical spectrum has historically shown no broad components on the emission lines, nor does spectropolarimetry show any broad-line-region visible in scattered light (Heisler, Lumsden and Bailey 1997). The latter classification is based upon its brightness in the 2-10 keV band, which led to its detection in early hard X-ray surveys (Ward et al. 1978).

An *ASCA* observation of NGC 7582 showed a complex spectrum in the 0.5-10 keV band, composed of a heavily absorbed ($N_H \sim 10^{23} \text{cm}^{-2}$) and flat ($\Gamma \sim 1.4$) continuum, plus an unabsorbed and steep component dominating below 2 keV (Turner et al 1997). The hard component shows flux variations down to timescales of a few thousand seconds (Turner et al. 1997; Schachter et al 1998; Xue et al 1998) confirming its association with an active nucleus in this source. Xue et al (1998) report a significant change in X-ray spectrum between the 1994 and 1996 *ASCA* observations of NGC 7582. The spectral change was consistent with an increase of the X-ray column by $\sim 4 \times 10^{22} \text{cm}^{-2}$ between these epochs, indicating that the X-ray absorber is not a simple uniform screen (Xue et al 1998). A variation in X-ray absorption was previously suggested based upon comparison between *Einstein*, *EXOSAT* and *Ginga* spectra of NGC 7582 (Warwick et al. 1993). The soft X-ray flux has shown no evidence for rapid variability to date. The soft flux is most likely composed of contributions from the active nucleus of NGC 7582, from starburst regions or other hot gas in the host galaxy and from spatially-unresolved nearby X-ray sources.

Aretxaga et al. (1999; hereafter A99) report observations of NGC 7582 in a very unusual optical state during July of 1998 when the Seyfert showed the presence of strong and broad line components blueshifted by $\sim 2500 \text{ km s}^{-1}$ relative to the narrow components. A99 report the width of $\text{H}\alpha$ to be $\text{FWHM} \sim 12000 \text{ km s}^{-1}$ and the flux state of the source to be relatively high at the time of this optical “event”. Following an IAU circular announcing an unusual optical state for NGC 7582, we performed optical and *BeppoSAX* observations in October and November of 1998, respectively.

2. The *BeppoSAX* Observation

BeppoSAX (Boella et al. 1997a) observed NGC 7582 over the period 1998 November 9 – 10 and we report on data from the three co-pointed narrow-field-instruments: the Low and Medium Energy Concentrator Spectrometers (LECS and MECS, respectively), covering $\sim 0.1 - 10 \text{ keV}$ (Parmar et al. 1997) and $1.3 - 10 \text{ keV}$ (Boella et al. 1997b) and the Phoswich Detector System (PDS; Frontera et al. 1997) providing data over $\sim 13 - 200 \text{ keV}$. The full-band of each instrument can be used for construction of light curves and images, but in the spectral analysis (§2.3) only a subset of data are used; $0.1 - 4 \text{ keV}$ (LECS), $1.5 - 10 \text{ keV}$ (MECS) and $15 - 100 \text{ keV}$ (PDS). This observation was part of a large spectral survey program, but was brought forward to occur as close as possible to the unusual optical event.

Standard data reduction was performed using the SAXDAS software package version 2.0 following Fiore, Guainazzi & Grandi (1999). Data from MECS2 and MECS3 were combined, as were data from the four PDS phoswich units, after gain equalization and linearization. The instruments are switched off during SAA passages and PDS data acquired during the first 5 minutes after each SAA passage have been rejected to exclude periods of highly variable risetime threshold (see Fiore, Guainazzi & Grandi 1999). This exclusion reduces the total 13-200 keV background from 30 to about 20 ct s^{-1} and the 13-80 keV background from 20 to about 12 ct s^{-1} . The PDS rocking mode provides a very reliable background subtraction. This has been checked using the spectrum between 220 and 300 keV, where the effective area of the PDS to X-ray photons is negligible and therefore the source contribution is negligible. We obtain, after background subtraction, $0.014 \pm 0.012 \text{ counts s}^{-1}$ consistent with the expected value of 0.

Standard screening of the *BeppoSAX* data yielded events files with effective exposure times of 27.3 ks (LECS), 56.4 ks for the combined MECS2/3 instruments and 52.2 ks for the PDS. The LECS exposure is lower than that in the MECS because the former is switched off during periods when the Earth’s illuminated limb is close to the line-of-sight.

2.1. Contamination Issues

The LECS and MECS instruments have fields-of-view (*fov*) with radii $22'$ and $28'$ respectively, while the PDS has a collimated *fov* with $\text{FWHM} = 1.4$ degrees. The region around NGC 7582 contains numerous X-ray sources evident in the *BeppoSAX* data (Fig. 1). Catalogues available online (via the HEASARC) show 17 AGN exist within a 1.5 degree radius of NGC 7582, in addition to the cluster Sersic159-03. Of the AGN, the BL Lac PKS 2316-423 and the Seyfert NGC 7590 are brightest in the soft X-ray band. However, most of the sources in this field have a soft X-ray spectrum, as is evident by comparison of the left and right panels of Fig. 1. In fact, construction of a MECS image in the 5-10 keV range allows confirmation that none of the known AGN within the *fov* are detected above 5 keV, nor is there any other hard X-ray source of comparable flux to NGC 7582 within the MECS *fov*. There is a chance that a significant hard source may exist outside of the MECS *fov* but within the PDS collimator; however, there is no such known source.

As reported by Schachter et al (1998), there is a significant unidentified soft X-ray source detected at J2000 $23^h18^m29.9^s$, $-42^\circ20'41.4''$ in *ROSAT* HRI and PSPC images, i.e. about $2'$ from NGC 7582 and which we henceforth refer to as RX J231829.9-422041. During the 17.2 ks HRI observation Schachter et al (1998) found 225 ± 32 counts from NGC 7582 and 90 ± 26 counts from RX J231829.9-422041.

The proximity of RX J231829.9-422041 would be irrelevant if we could spatially resolve this source from NGC 7582 in the LECS and MECS data. The MECS have a spatial resolution of $1.2'$ (FWHM) at 6 keV, allowing the potential separation of any hard X-rays from the serendipitous source and NGC 7582. However the spatial resolution of the LECS is $3.5'$ at 0.25 keV, making separation difficult at the softest energies. Examination the LECS and MECS images (Fig. 1) shows evidence for a significant region of unresolved soft X-ray emission on the north-east side of NGC 7582, consistent with the position of RX J231829.9-422041. Unfortunately the LECS emission from RX J231829.9-422041 is not separable from the tail of the point-spread-function of LECS counts from NGC 7582. Thus we investigate the nature of RX J231829.9-422041, to determine whether we can quantify the contamination of the NGC 7582 data based on the *ROSAT* flux and spectrum.

Overlaying optical and X-ray images shows that RX J231829.9-422041 appears to lie outside of the host galaxy (which has a $\sim 5' \times 2.5'$ diameter on the sky, from the SKYVIEW digitized Southern Sky Survey plus Palomar Sky Survey E plates) and hence may be a foreground source or background quasar. We obtained a spectrum of an optical candidate at J2000 $23^h18^m29.94^s$, $-42^\circ20'40.7''$ using the 4m telescope at CTIO with RC spectrograph and Loral 3K CCD. The data were accumulated with a spectral resolution of 6.3 \AA over $\sim 4000 - 9000 \text{ \AA}$ and a WG360 blocking filter was used. Wavelength calibration utilized

a helium/argon spectrum yielding an accuracy of 3 Å. The data were extracted using standard methods and the IRAF software. The optical spectrum of RX J231829.9-422041 was flux-calibrated using standard star LTT9491 (Stone & Baldwin 1983; Baldwin & Stone 1984); target and standard star were observed close to the zenith using a 1.5" slit and under photometric conditions.

The spectrum was accumulated UT 1998 October 17 and we show the data binned to a resolution of 8 Å over the $\sim 4500 - 9000$ Å bandpass (Fig. 2). An unresolved line is evident at 6593 Å and a broad line at 8638 Å. The presence of a strong broad line (FWHM width $\sim 3000 \text{ km s}^{-1}$) indicates the source is an AGN. Assuming the broad line is $\text{H}\alpha$ then the redshift is $z=0.316$ and the 6593 Å line is consistent with $[\text{OIII}] \lambda 5007$. $\text{H}\beta$ is expected at 6397 Å but not observed, this could be relatively weak and hidden in the noise. However, Schachter et al (1998) note another, fainter, optical candidate within the HRI error box, for which we have no optical spectrum, thus the identification of the X-ray source remains inconclusive.

We compared the X-ray flux of RX J231829.9-422041 during the PSPC and HRI observations and found $F_{0.1-2} = 8.7 \pm 1.0 \times 10^{-14}$ and $1.4 \pm 0.40 \times 10^{-13} \text{ erg cm}^{-2} \text{ s}^{-1}$ respectively, assuming the model noted below. A 58% increase is seen between the two observations, which are separated by ~ 2 years, consistent with the tentative AGN identification. If the optical source is the correct counterpart of RX J231829.9-422041, then for a redshift $z=0.316$, the luminosity is $L_{0.1-2} = 3.6 \times 10^{43} \text{ erg s}^{-1}$.

Thus we conclude RX J231829.9-422041 is likely to be an AGN, and the source variability makes contamination in the LECS data a problem. To minimize contamination we choose a special extraction cell for the LECS data from NGC 7582. The standard LECS extraction cells of 8' or 4' would include some contaminating emission from these sources, as is evident from Fig. 1. To minimize contamination of the soft spectrum we choose a LECS extraction cell using sky coordinates which allows selection of spectral counts only from the south-west semi-circle of a circular region centered on the nucleus of NGC 7582. The position angle for the dividing line was 128 degrees, measured anti-clockwise from North. This was properly scaled to reflect its contribution of only half the normal LECS flux, and provides the least contaminated LECS spectrum possible.

2.2. Timing Analysis

Fig. 3 shows the light curves of NGC 7582 sampled with 5000 s bins, in different bandpasses. The LECS on-source light curve was extracted from the semi-circular region

described above, and hence represents only half of the LECS count rate of the source in a standard 8' circle in the 0.1–1 keV bandpass. The LECS background light curve is also shown. No significant variability is detected in the 0.1–1 keV band ($\chi^2 = 17.9/17 \text{ dof}$). The MECS light curve shows short-term variability in the 5–10 keV flux, with factor of two variations on timescales of $\sim 15,000$ s and lower amplitude variability occurring on timescales of a few thousand seconds. The MECS background level is negligible and not shown. The PDS light curve is shown in the 13–60 keV band, and appears consistent with the MECS light curve (although we are not sensitive to small lags). This indicates that the PDS data for NGC 7582 are not significantly contaminated by any other source. Furthermore, the similarity in 5–10 and 13–60 keV light curves indicates that the emission in those bands originates in the same physical component, or in very closely linked regions (see next section).

NGC 7582 yielded 0.013 ± 0.008 source ct/s in the LECS (0.1 – 4 keV band; this is the rate in the half-cell so should be doubled for comparison with other sources), 0.166 ± 0.002 ct/s in the MECS (1.5 – 10 keV) and 0.82 ± 0.04 ct/s in the PDS (15 – 100 keV) corresponding to fluxes $F_{0.5-2} = 5.66 \times 10^{-13} \text{ erg cm}^{-2} \text{ s}^{-1}$, $F_{2-10} = 1.97 \times 10^{-11} \text{ erg cm}^{-2} \text{ s}^{-1}$, $F_{10-100} = 1.16 \times 10^{-10} \text{ erg cm}^{-2} \text{ s}^{-1}$ for the best-fitting model (see §2.3). Uncertainties in absolute flux calibration are $\sim 15\%$.

2.3. Spectral Analysis

Spectral data were extracted from a circular region of radius 4' for the MECS, chosen to encircle $\sim 90\%$ of the source counts. The LECS data were taken from a co-centered semi-circle of radius 8', as described in detail in §2.1. LECS and MECS background spectra were taken from blank fields, using the same region of the detector in each case. It has been determined that this method of extracting background spectra yields a superior result to that obtained using an offset region from the source events file because the LECS and MECS background strongly varies with position in the detector.

In this section the *BeppoSAX* data were fit with the normalization of the MECS dataset fixed at 1; the PDS data were allowed a normalization in the range 0.75–0.85 (0.8 is the expected value found from fitting calibration sources). The LECS normalization was allowed to vary freely and was usually close to 0.45 (usually 0.9, but we have only half the source flux as noted above). Corrections for the source flux falling outside of the extraction cell due to the instrument point-spread-function were incorporated into the ARF files used in the spectral fitting.

2.3.1. The 3-100 keV Continuum

First, the *BeppoSAX* data were fit in the limited range of 3-5 keV plus 7-100 keV, using a single absorbed powerlaw model. This was to ascertain whether the continuum could be modeled in a simple way, when the complex soft emission and the iron $K\alpha$ line band were excluded. This model proved inadequate yielding $\chi^2 = 101/60$ *dof* and $\Gamma \sim 1.46$. The ratio of data/model (Fig. 4) shows data in the PDS band do not lie on the extrapolation of the continuum fitted to data from below 10 keV, suggesting the presence of an additional spectral component above 10 keV.

There are several models which can be tried. First, a complex absorber was fit to the data. The absorber component of the model was changed to a “dual-absorber”, whereby lines-of-sight to the continuum pass through one or both absorbers. This model yielded a good fit with $\chi^2 = 59/58$ *dof*. The data are described by a continuum of photon index $\Gamma = 1.95$ of which 60% is covered with a column $N_H = 1.60^{+0.94}_{-0.46} \times 10^{24} \text{cm}^{-2}$ and 100% is covered by $1.44^{+0.09}_{-0.10} \times 10^{23} \text{cm}^{-2}$; hereafter these absorbing components are referred to as the “thick absorber” and the “full screen”, respectively.

Some alternative parameterizations were tried for the hard spectral component. A reflection component was added to the model in place of the heavily absorbed fraction of powerlaw. The XSPEC PEXRAV model was used, representing reflection from neutral material (here assumed to be viewed at an angle $\cos\theta = 0.45$ to the line-of-sight) of Magdziarz & Zdziarski 1995. First the reflection component was assumed to be attenuated by the same column affecting the continuum, yielding $\chi^2 = 52/59$ *dof* and a solid angle of $\Omega/2\pi = 6.0$ steradians. If the PDS data were dominated by reprocessed emission from a geometrically large reflector then the PDS light curve would be expected to be smeared and lagged relative to the primary light curve. However, such large solid angles may have no geometrical meaning but may indicate anisotropy of the nuclear radiation. A test of the latter model is the consistency between the strengths of the iron line and reflection hump. In fact the reflection component is inconsistent (at $> 99\%$ confidence) with the strength of the iron $K\alpha$ line (George & Fabian, 1991). We reach the same conclusion if the reflection component suffers no absorption (except Galactic, $N_H = 1.47 \times 10^{20} \text{cm}^{-2}$, Stark et al. 1992). We conclude the hard component in NGC 7582 is not dominated by Compton reflection of the primary continuum.

We also tried a model where the hard X-ray spectrum suffers an exponential cutoff, to explain the spectral shape above 10 keV. When left unconstrained the cutoff energy reaches a solution beyond the upper limit of the PDS bandpass, rejecting the cutoff as a significant model parameter. When the cutoff energy was constrained to match the apparent turnover evident in the data (around a few tens of keV) then the continuum powerlaw was found

to be very flat $\Gamma \sim 1$ and the fit was inferior ($\chi^2 = 101/59 \text{ dof}$) to that found for the complex absorber model described above. Thus the dual-absorber model is favored over an exponentially cutoff powerlaw.

2.3.2. *The soft X-ray continuum*

In the previous section we found the best description of the 3-100 keV continuum to be a $\Gamma = 1.95$ powerlaw, 60% of which is absorbed by a column $N_H = 1.60 \times 10^{24} \text{cm}^{-2}$ (the thick absorber) and 100% by $1.44 \times 10^{23} \text{cm}^{-2}$ (the full screen). Extrapolation of this model below 3 keV reveals the soft X-ray data to be in excess of the model, and underlines the requirement for an additional component to parameterize the soft emission. To this end, a MEKAL component (assuming cosmic abundances) was added to the dual-absorber model detailed above, absorbed by a column fixed at the Galactic line-of-sight value $N_H = 1.42 \times 10^{20} \text{cm}^{-2}$. MEKAL is a model for the emission spectrum from collisionally ionized gas (Kaastra, 1992 and references within). At this stage, the iron line band of 5.0-7.0 keV remained excluded.

This model did not adequately describe all of the soft emission, yielding $\chi^2 = 153/134 \text{ dof}$, and so an additional component was added, representing an unabsorbed fraction of the hard X-ray continuum powerlaw. The soft flux can be attributed to a MEKAL component of temperature $kT = 0.72^{+0.29}_{-0.15} \text{keV}$. The unabsorbed powerlaw comprises $\sim 0.4\%$ of the continuum (the so-called full screen may cover only 99.6% of the nucleus, or this flux may arise outside of the full screen). In this fit $\chi^2 = 139/132 \text{ dof}$ and the MEKAL component accounts for 41% of the total 0.1 – 2 keV flux (Fig. 5). The total luminosity in the 0.1 – 2 keV band is $L_{0.1-2} \sim 4 \times 10^{40} \text{erg s}^{-1}$ at the redshift of NGC 7582. A second MEKAL component does not provide an adequate alternative to the “leaking” unabsorbed powerlaw component.

2.3.3. *The iron $K\alpha$ line*

With the acceptable dual-absorber model, we returned the 5.0-7.0 keV data to the spectral fit and turned to an examination of the iron $K\alpha$ line. If the model allowed an unconstrained line width then the line went to the maximum allowed width of 1 keV. The line can be difficult to parameterize if the continuum is complex, and we considered the possibility that we still have not achieved a correct absorption model for this source, in which case the source might show some unmodeled absorption from the K edge of iron. It

is important to establish whether we have adequately parameterized the absorber because otherwise confusion arises between which are line and continuum photons. However, addition of an edge to the model did not significantly improve the fit.

Given that the line is quite faint, we tried fits fixing the width at values of $\sigma = 0.41$ keV (to compare with the *ASCA* fit), 0.0 keV (to examine the parameterization as a narrow line) and the intermediate value of 0.2 keV (to expand our examination of parameter-space). With $\sigma = 0.41$ the fit yields a line at rest-energy $6.15^{+0.50}_{-0.65}$ keV and $\chi^2 = 149/150$ *dof*. The data and residuals for the dual-absorber fit including this iron $K\alpha$ line are shown in Fig. 5, along with the model. If we assume the line and continuum are both absorbed then the line equivalent width is $EW = 186^{+114}_{-79}$ eV (absorption-corrected line against absorption-corrected continuum). With $\sigma = 0.2$ we obtain a rest-energy $6.24^{+0.29}_{-0.33}$ keV, $EW = 125^{+77}_{-77}$ eV and $\chi^2 = 153/150$ *dof*. If the line is assumed to be narrow ($\sigma = 0$) then we obtain $EW = 90^{+57}_{-40}$ eV and $\chi^2 = 157/150$ *dof*. Alternatively, if we assume the iron line is not absorbed, then the narrow Gaussian fit produces $EW = 570^{+570}_{-120}$ eV against the absorbed continuum level. In realistic physical models the line is produced within the absorbing clouds, not in front of or behind them as in our parameterizations. Despite this shortcoming we can make a crude comparison with the line EW predicted by transmission of X-rays through a sphere of the thick absorber, which would be several keV (Leahy and Creighton, 1993). The full screen of gas should produce a narrow line of $\sim 100 - 150$ eV. However, the preference for a broad line in these data suggests relativistic effects may be important, inferring an origin for the line close to the black hole.

2.4. Comparison with the *ASCA* data

The *BeppoSAX* data were compared with the best-fitting double-powerlaw solution found for the *ASCA* 1994 data (with hard photon index $\Gamma = 1.38$, absorbed by column $N_H = 7.4 \times 10^{22} \text{cm}^{-2}$, plus soft unabsorbed component parameterized by $\Gamma = 2.68$; Turner et al. 1997). First the *ASCA* model was compared to the data with no refitting or re-normalization, and the data/model ratio is shown in Fig. 6a. Clearly the AGN has brightened in the hard and soft bands since 1994 with evidence for a larger absorption at the *BeppoSAX* epoch. Our choice of extraction region for the LECS should reduce contamination of NGC 7582 by the north-east sources and so this change in soft flux is most likely closely associated with the nucleus. The *ASCA* data were probably contaminated by significant flux from RX J231829.9-422041. However, the fact the uncontaminated soft flux measurement of NGC 7582 by *BeppoSAX* is *higher* than the *ASCA* measurement means a significant soft flux increase must have occurred in NGC 7582.

There is a dip at 6 keV but this does not represent a significant difference in the flux of the iron $K\alpha$ line because the *ASCA* 1994 measurement of this line (Turner et al 1997) had an uncertainty of a factor ~ 2 . Fig 6b compares the *BeppoSAX* spectra with the second *ASCA* observation, from 1996, finding NGC 7582 brighter during the 1998 *BeppoSAX* observation. Fig. 6c shows a comparison between the two *ASCA* observations. Significant changes in absorbing column are evident between the two *ASCA* observations, as reported in detail by Xue et al. (1998) and previously noted in this source (Warwick et al. 1993), similarly, column changes are evident between the *ASCA* and *BeppoSAX* epochs. Of course, the effect of a column as large as $\sim 10^{24}\text{cm}^{-2}$ is not detectable below 10 keV and the column variations evident in the *ASCA-ASCA* and *ASCA-BeppoSAX* comparisons occur in the full screen.

Flux variability is also observed on long and short timescales in the hard band, and on long timescales in the soft X-ray band. A limitation of plots such as Fig. 6 is the absence of an indication of the uncertainty in the *ASCA* model, to which we compare the *BeppoSAX* data. Thus we provide the ratio of the *ASCA* 1994 data to the best-fitting model to those 1994 data (Fig. 6d) to give an idea of the (small) residual uncertainty in the *ASCA* fit. To conclude, *BeppoSAX* data provide evidence for a more complex spectrum than previously known for this source; furthermore, significant flux, column (full screen) and index variability are evident on timescales of years.

Next we tried to parameterize the long-term spectral changes by application of the *BeppoSAX* dual-absorber model to the 1994 November *ASCA* data. Data from 1994 appear most dramatically different to the spectrum at the *BeppoSAX* epoch and, as the differences between the two *ASCA* observations are discussed by Xue et al. (1998), we concentrate on this 1998 to 1994 comparison.

2.4.1. Comparison of X-ray Spectra from 1994 and 1998

Fitting the *ASCA* data from the 1994 observation with the *BeppoSAX* model we found that the spectral variability between 1998 and 1994 could not be explained by a simple change of one spectral parameter. Further analysis showed it could not be understood by allowing the column densities of the thick absorber and/or full screen to vary even if both covering fractions were also free.

As the spectral variability appears complex, the *ASCA* data were refit with the *BeppoSAX* model, this time allowing all spectral parameters to vary. This fit yielded a spectral index of $\Gamma = 1.55^{+0.19}_{-0.15}$, column of $N_H = 7.64^{+0.86}_{-0.68} \times 10^{22}\text{cm}^{-2}$. These values agree

with similar fits to the *ASCA* data obtained by Turner et al. (1997). Thus the photon index appears to have steepened by $\Delta\Gamma = 0.40$ between 1994 and 1998, while the full screen has increased by $\Delta N_H \sim 7 \times 10^{22} \text{cm}^{-2}$. The fit gave $\chi^2 = 509/392 \text{ dof}$, with no systematic residual.

The change in soft flux can be modeled as an increase in normalization of the MEKAL component by a factor $2.2^{+1.2}_{-0.6}$. The unabsorbed fraction of powerlaw was consistent with that found at the *BeppoSAX* epoch, as was the MEKAL temperature, and all parameters of the iron $K\alpha$ line (albeit poorly constrained).

We considered whether the full screen might be partially-ionized, however such models found no better fit than those presented here, and given the difficulty in separating nuclear and starburst components below 2 keV, we do not pursue this further. It is evident that significant flux and column changes occur closely associated with the nucleus of NGC 7582, but the spectral changes are complex.

3. The Optical Spectrum

An optical spectrum of NGC 7582 was obtained on UT 1998 October 17 (Fig. 7) using the CTIO 4m telescope with the setup as described in §2.1. NGC 7582 was flux-calibrated using standard star LTT9491 (Stone & Baldwin 1983; Baldwin & Stone, 1984) both of which were observed close to the zenith using a $1.5''$ slit, under photometric conditions. NGC 7582 was observed for a total exposure time 1200 s. The 1998 Oct 17 spectrum shows a broad component on $H\alpha$, with width $\text{FWHM} = 6400 \text{ km s}^{-1}$, and a peak indicating a redshift of $\sim 590 \text{ km s}^{-1}$ relative to the narrow lines. We find our line widths in good agreement with those found by A99 for 1998 Oct 21, and concur that at this epoch, the broad line showed a slight redshift relative to the narrow lines.

4. Discussion

Interest in the *BeppoSAX* X-ray spectrum is twofold; providing spectral constraints on NGC 7582 up to 100 keV, and providing an X-ray spectrum which offers clues to the nature of a significant and unusual optical event associated with the nuclear regions.

4.1. The X-ray Results

First we summarize the new X-ray results. *BeppoSAX* reveals a hard X-ray component, peaking at ~ 20 keV, previously unknown in this source. By now, *BeppoSAX* has discovered numerous examples of continuum components visible only above 10 keV, for example NGC 1068 (Matt et al. 1997); NGC 3393 and NGC 4941 (Salvati et al. 1997); Mrk 3 (Cappi et al 1999); NGC 2110 (Malaguti et al 1999) and Circinus (Matt et al. 1999). In some cases the hard component has been found to be consistent with Compton Reflection of the continuum while in others a heavily absorbed ($N_H > 10^{24}\text{cm}^{-2}$) fraction of the primary continuum is suggested. For NGC 7582 we prefer the latter model. We find variability in the flux above 10 keV on timescales down to a few thousand seconds, correlated with that seen below 10 keV. Combined with the spectral result this suggests that a powerlaw continuum of photon index $\Gamma = 1.95$ dominates from 2 – 100 keV. This continuum is transmitted through a “thick absorber” with a column $N_H = 1.60_{-0.46}^{+0.94} \times 10^{24}\text{cm}^{-2}$ covering 60% of the nucleus plus a “full screen” covering 100% of the source with $N_H = 1.44_{-0.10}^{+0.09} \times 10^{23}\text{cm}^{-2}$. The *BeppoSAX* model for NGC 7582 can be extrapolated to 150 keV and compared with the OSSE measurement of flux (taken from data summed from observations spanning 1991-1994). We find for *BeppoSAX* $F_{50-150\text{ keV}} = 6.88 \times 10^{-11}\text{erg cm}^{-2}\text{s}^{-1}$ and for OSSE $F_{50-150\text{ keV}} = 3.84_{-0.56}^{+1.06} \times 10^{-11}\text{erg cm}^{-2}\text{s}^{-1}$ (Johnson et al 1994) thus *BeppoSAX* finds NGC 7582 significantly brighter ($\sim 80\%$) than the average flux-state sampled by OSSE data summed from observations in 1991, 1992 and 1994. Alternatively the spectrum may cut-off sharply above 50 keV, leading to an overestimate of flux when extrapolating the *BeppoSAX* spectrum up to 150 keV.

In NGC 7582 *BeppoSAX* data provide some insight into the geometry of the X-ray absorber. There are several models which would allow observation of a nuclear source through differing column densities. However, a single absorber which is thick at the center and tapered towards the edges would produce a smooth range of columns from center to edge. This would look like a flat spectrum, rather than show the relatively sharp turn-over seen in the 5 – 10 keV band (Fig. 5). A similar spectrum is expected from a nuclear source viewed through a distribution of many clouds of varying column densities. Thus the data provide strong evidence against those geometries. The measured columns and fractions are consistent with a thick absorber composed of a single cloud, or several clouds with $N_H \sim 1.6 \times 10^{24}\text{cm}^{-2}$ covering $\sim 60\%$ of the nuclear source. The screen with $N_H \sim 1.4 \times 10^{23}\text{cm}^{-2}$ fully covers the source. The location of the full screen relative to the thick cloud(s) is unknown. The thick absorber will provide an optical depth of ~ 1 to electron scattering. Any quasi-spherical distribution of such clouds will result in the introduction of smearing and lags of the intrinsic variations in the nuclear light curve. However, the absence of very sharp flux variations, and the uncertainty as to the intrinsic

light curve do not allow us to place any constraints on the basis of the flux variability observed.

The absorber in NGC 7582 can be compared to the complex absorbers found in some other Seyfert galaxies. NGC 2110 (Malaguti et al. 1999) and IRAS 04575-7537 (Vignali et al. 1998) show 30% covering by a column $\sim \text{few} \times 10^{23} \text{cm}^{-2}$ plus full-covering by $\sim \text{few} \times 10^{22} \text{cm}^{-2}$ and so in comparison NGC 7582 has an order of magnitude higher column in each component. Seyfert 1 galaxies may have a similarly complex geometry of circumnuclear absorption, but with gas of much higher ionization state. Several Seyfert 1 galaxies have shown evidence for two zones of absorbing gas with differing ionization-state (e.g. Kriss et al. 1996; George et al. 1998).

Comparison with previous *ASCA* observations allows us to look for changes in the full screen. Application of the *BeppoSAX* model to the *ASCA* data suggest a steepening of the photon index by $\Delta\Gamma = 0.40$ and an increase of column by $\Delta N_H \sim 7 \times 10^{22} \text{cm}^{-2}$ between 1994 and 1998. If changes in column and index are connected, then changes in the circumnuclear absorption could be linked to changes in the region which Compton upscatters nuclear photons. As discussed by Xue et al. (1998), assuming column changes are caused by transverse passage of inhomogeneities in the absorber crossing the line-of-sight, then the minimum timescale for column variations (i.e. that found between the two *ASCA* observations) can be used to obtain a limit to the radial distance from the nucleus and clump sizes within the absorber. Xue et al. (1998) conclude the full screen to be consistent with the putative torus.

It is unclear whether any small fraction of the nuclear continuum escapes without attenuation, the unabsorbed soft X-rays that we observe could arise from starburst regions outside of the absorber. The X-ray emission from starburst and AGN cannot be separated spatially or spectroscopically using these X-ray data.

4.2. The relation between Optical and X-ray Properties

Now we examine the *BeppoSAX* results in light of the recent optical brightening and the development of broad components to some permitted lines sometime between 1998 June 20 (Halpern, Kay & Leighly 1998) and 1998 July 11 (A99). The constant optical centroid of NGC 7582 (within an error radius of 12 pc) indicates that this “event” was closely associated with the nucleus (A99). Our optical spectrum is in agreement with October 1998 spectra shown by A99, confirming their result that NGC 7582 had returned to close to its typical “type 2” characteristics by 1998 October, although with some obvious broad

component remaining on $H\alpha$.

To review the recent X-ray flux history of NGC 7582: *ASCA* observations showed $F_{2-10} = 1.51 \times 10^{-11}$ and $1.82 \times 10^{-11} \text{erg cm}^{-2}\text{s}^{-1}$ during 1994 November and 1996 November, respectively. A *RXTE* observation during 1998 October revealed $F_{2-10} = 9.5 \times 10^{-12} \text{erg cm}^{-2}\text{s}^{-1}$ (Takeshima, p.comm). This *BeppoSAX* observation shows $F_{2-10} = 1.97 \times 10^{-11} \text{erg cm}^{-2}\text{s}^{-1}$. We conclude that NGC 7582 was not in an obvious prolonged X-ray high-state after the optical event. In fact comparison between *RXTE* and *BeppoSAX* revealed a doubling of X-ray flux between 1998 October and November, while the optical flux continued to decline by 30% between 1998 October 6 and 21 (A99).

In the context of the *BeppoSAX* model for the X-ray absorber, the broad optical permitted lines must originate somewhere within the full screen, which has sufficient opacity to hide those lines from view. The appearance of broad components on the permitted lines is explained if holes appear in the full screen. This does not require the full screen to lie outside of the thick absorber, because 40% of the line-of-sight is clear of the thick absorber, thus holes in the full screen would lead to some clear lines-of-sight to the broad-line-region. Holes or changes of opacity could occur if material forming the full screen is inhomogeneous and is moving relative to the line-of-sight. If we attribute the optical changes in NGC 7582 to holes appearing in the full screen then we also expect measurable changes in optical reddening to be observed. This scenario has been previously suggested to explain similar changes in the optical spectra of Mrk 993 and Mrk 1018 (Goodrich 1989, 1995 respectively). A99 find the observed variations in the optical spectrum to be inconsistent with a simple decrease in optical reddening. However, as noted by A99, the gas and dust in NGC 7582 may result in a different reddening law than that assumed and even more importantly the starburst “contamination” of nuclear spectrum has to be removed, this has been done in the absence of high-spatial-resolution spectroscopy leaving some uncertainty in the optical reddening results. We feel these uncertainties leave open the possibility of a change in the full screen leading to the observed events. The soft-band X-ray flux appears highly variable on timescales of years, consistent with a model where the full screen allows a variable amount of continuum leakage. However, as noted above, the origin of the soft flux itself is ambiguous and there are other possible explanations for an increase of this kind (variation in a spatially-unresolved source close to the nucleus, for example).

A99 discuss another explanation for the behavior of NGC 7582, suggesting the broad line components were produced in a SN IIn explosion, these can produce broad lines without P-Cygni profiles (Schlegel, 1990). Starburst activity is important close to the nucleus of this source (Oliva et al 1995) and so a supernova event could occur so close to the nucleus as to be spatially unresolved from it, and could also produce the observed increase in soft

X-ray flux. A99 compare the evolution of the optical spectrum (widths of the broad line components) of NGC 7582 to that of the SN IIn SN 1988Z, finding good agreement. Our optical data also lie on the A99 evolutionary curve (for line width).

4.3. The Big Picture

The detection of hard components, such as that found in the *BeppoSAX* data of NGC 7582, are of great interest with regard to the question of the true intrinsic luminosity of type 2 Seyferts. Taking the *BeppoSAX* model, and calculating the *unabsorbed* 2–10 keV luminosity yields $L_{2-10} = 10^{43} \text{ erg s}^{-1}$, a factor of several higher than the luminosity inferred from the *ASCA* measurements. As pointed out by Matt et al (1999) these hard components peak at a few tens of keV, the same energy as the cosmic X-ray background. The spectra of many other Seyferts also appear flat when viewed in the 2–10 keV bandpass, e.g. NGC 2110 (Hayashi et al 1996; Malaguti et al. 1999), NGC 5252 (Cappi et al 1996), IRAS 04575-7537 (Vignali et al. 1998) and NGC 7172 (Guainazzi et al 1998). These flat spectra and the evidence for “excess iron K edges” in several NELGs (Turner et al. 1997) indicates that complex absorption is a widespread phenomenon and the X-ray flux above 10 keV is likely significantly underpredicted for the Seyfert population when extrapolating the spectrum from lower energies. Thus *BeppoSAX* results from flat-spectrum Seyferts indicate that more of the X-ray background could be attributed to Seyfert 2s and NELGs than previously thought.

5. Conclusions

A *BeppoSAX* observation of NGC 7582 reveals a previously unobserved hard X-ray spectral component visible above 10 keV. Correlated variability above and below 10 keV suggest that a single continuum component dominates the 2 – 100 keV band. Comparison with *RXTE* data shows the flux in the 2 – 10 keV band has varied by factors of several in the last few months, thus the nuclear flux appears not to be correlated with the gradual decline noted in optical flux which followed the unusual optical event of July 1998. The 0.5 – 2 keV flux has brightened by a factor ~ 2 since 1994, and this flux change seems most likely closely associated with the nucleus of NGC 7582.

The $\sim 2 - 100$ keV spectrum can be parameterized by a powerlaw of photon index $\Gamma = 1.95$ which is significantly steeper ($\Delta\Gamma = 0.40$) than an *ASCA* measurement of four years earlier. The X-ray absorber can be modeled as two distinct zones, a thick absorber

with $N_H \sim 1.6 \times 10^{24} \text{cm}^{-2}$ covering $\sim 60\%$ of the nuclear source plus a full-covering screen $N_H \sim 1.4 \times 10^{23} \text{cm}^{-2}$. An absorber which is thick at the center and tapered towards the edges, and a distribution of clouds of differing column densities are geometries which are strongly disfavored by the data. The column density of the full screen appears to have increased by $\Delta N_H \sim 7 \times 10^{22} \text{cm}^{-2}$ over the last four years. This result confirms the previous finding of column variability in this source (Xue et al 1998, Warwick et al. 1993).

It is possible that observed increases in soft X-ray flux over timescales of years are due to the appearance of holes in the full screen of the X-ray absorber, allowing a small leakage of the nuclear continuum (at the level of $\sim 1\%$ or less). However, it is difficult to discern the relative contributions to the soft X-ray flux from the active nucleus and any outburst in the starburst regions of the host galaxy. Thus these data are also consistent with the suggestion by Aretxaga et al (1999) that the radiative onset of a type IIIn supernova caused the observed change in properties of NGC 7582.

6. Acknowledgements

We thank the *BeppoSAX* satellite operations team. This research has made use of SAXDAS linearized and cleaned event files produced at the *BeppoSAX* Science Data Center. We also thank M. Cappi, F. Haardt for useful comments. Thanks to Itziar Aretxaga and coauthors for providing their paper on the optical observations of NGC 7582 prior to publication, also to Lorella Angelini for useful discussions about the data reduction, Steve Kraemer for bringing the IAU circular to our attention, Mike Crenshaw for help with reduction of the optical data and the anonymous referee for useful comments.

Table 1. *BeppoSAX* and *ASCA* Parameters

	Flux _{0.5–2} 10 ^{–13} erg cm ^{–2} s ^{–1}	Flux _{2–10} 10 ^{–11} erg cm ^{–2} s ^{–1}	Γ	N_H^{FS} ^a 10 ²³ cm ^{–2}	N_H^{TA} ^b 10 ²³ cm ^{–2}	χ ² / <i>dof</i>
SAX	5.66 ^{+0.85} _{–0.85}	1.97 ^{+0.3} _{–0.3}	1.95 ^{+0.09} _{–0.18}	1.44 ^{+0.09} _{–0.10}	16.00 ^{+9.40} _{–4.60}	59/58
A94 ^c	3.63 ^{+0.49} _{–0.67}	1.51 ^{+0.36} _{–0.42}	1.33 ^{+0.16} _{–0.16}	0.75 ^{+0.05} _{–0.04}	...	300/288
A96 ^c	4.18 ^{+0.34} _{–0.40}	1.55 ^{+0.24} _{–0.22}	1.52 ^{+0.13} _{–0.13}	1.20 ^{+0.11} _{–0.08}	...	601/578

^aFS is the full screen absorber completely covering the nucleus

^bTA is the thick absorber covering 60⁺¹⁰_{–14}% of the nucleus

^c*ASCA* results from 1994 and 1996 taken from Xue et al. 1998, from their Table 1, fit 2

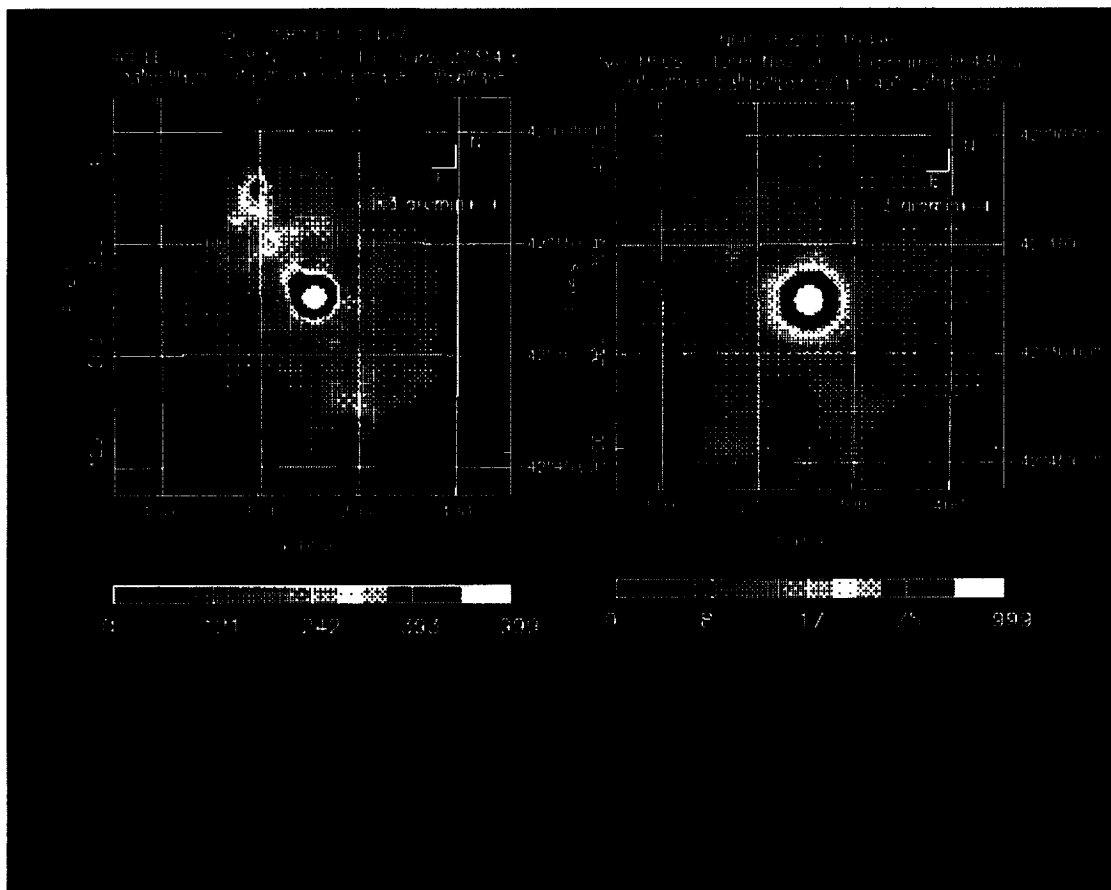


Fig. 1.— The smoothed LECS and MECS images in the 0.1 – 2 keV and 5-10 keV bands, respectively. Extended emission and several nearby X-ray sources are evident in the LECS band, but none of the serendipitous sources provide significant flux above a few keV.

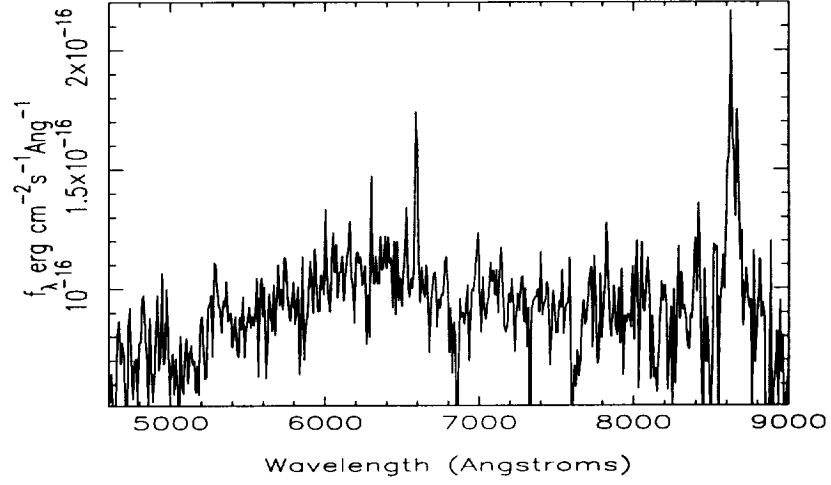


Fig. 2.— The optical spectrum of RX J231829.9-422041 which is 2' away from NGC 7582. Dropouts close to 6860Å and 8870Å are instrumental effects due to charge traps in the CCD. The broad line observed at 8638Å is likely to be H α at $z=0.316$, the line observed at 6593Å is then identified as [OIII] λ 5007.

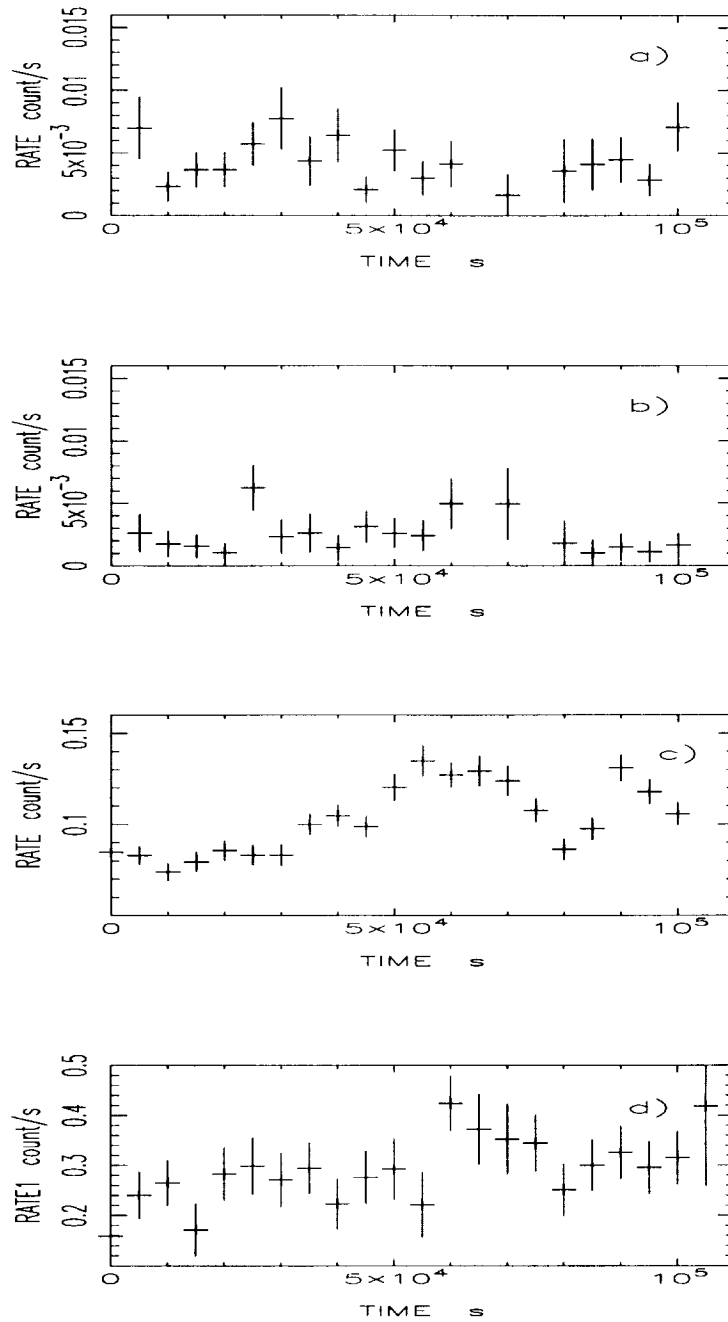


Fig. 3.— The LECS source (a) and background (b) light curves in the 0.1-1 keV band; c) MECS light curve from the 5-10 keV band and (d) the PDS light curve in the 13-60 keV band. All curves have 5000s bins, the MECS background rate is negligible and the PDS data have had the background level subtracted.

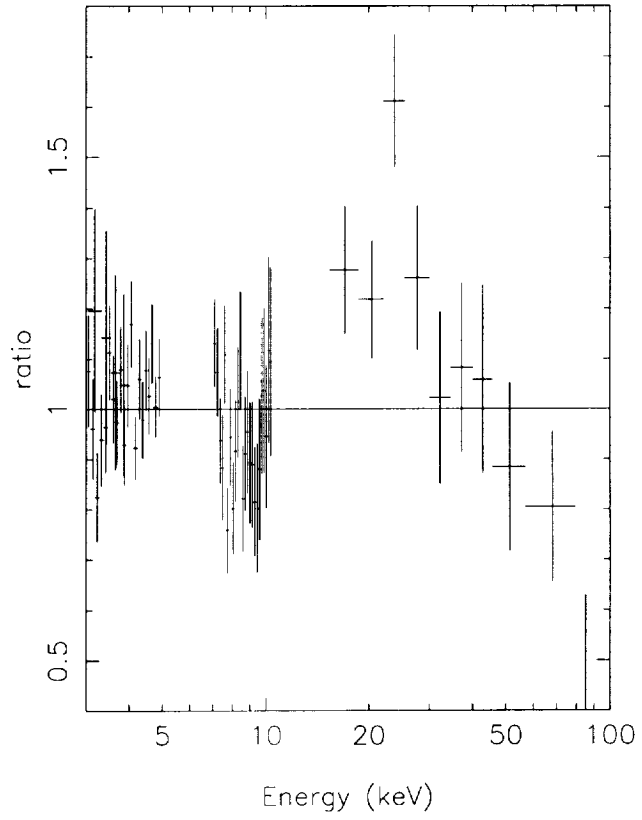


Fig. 4.— *The BeppoSAX data from 3-5 keV plus 7-100 keV compared to a simple model of an absorbed powerlaw.*

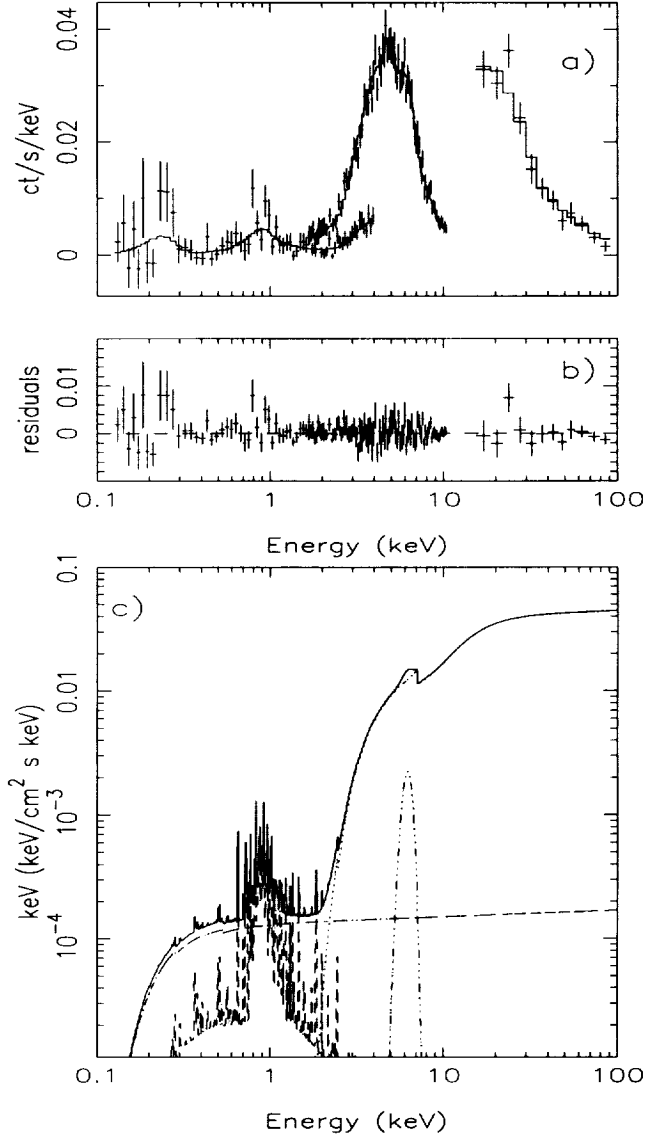


Fig. 5.— *The BeppoSAX data (a) and residuals (b) compared to the best-fitting dual-absorber model (c). The solid line shows the sum of all components. The dotted line shows the powerlaw continuum, the turnover at ~ 20 keV is due to the thick absorber and the turnover evident at a few keV is due to the full screen. The effects of the Galactic column become evident at ~ 0.4 keV. The dashed line shows the MEKAL component, the dash-dot lines show the iron $K\alpha$ emission line and the unattenuated continuum.*

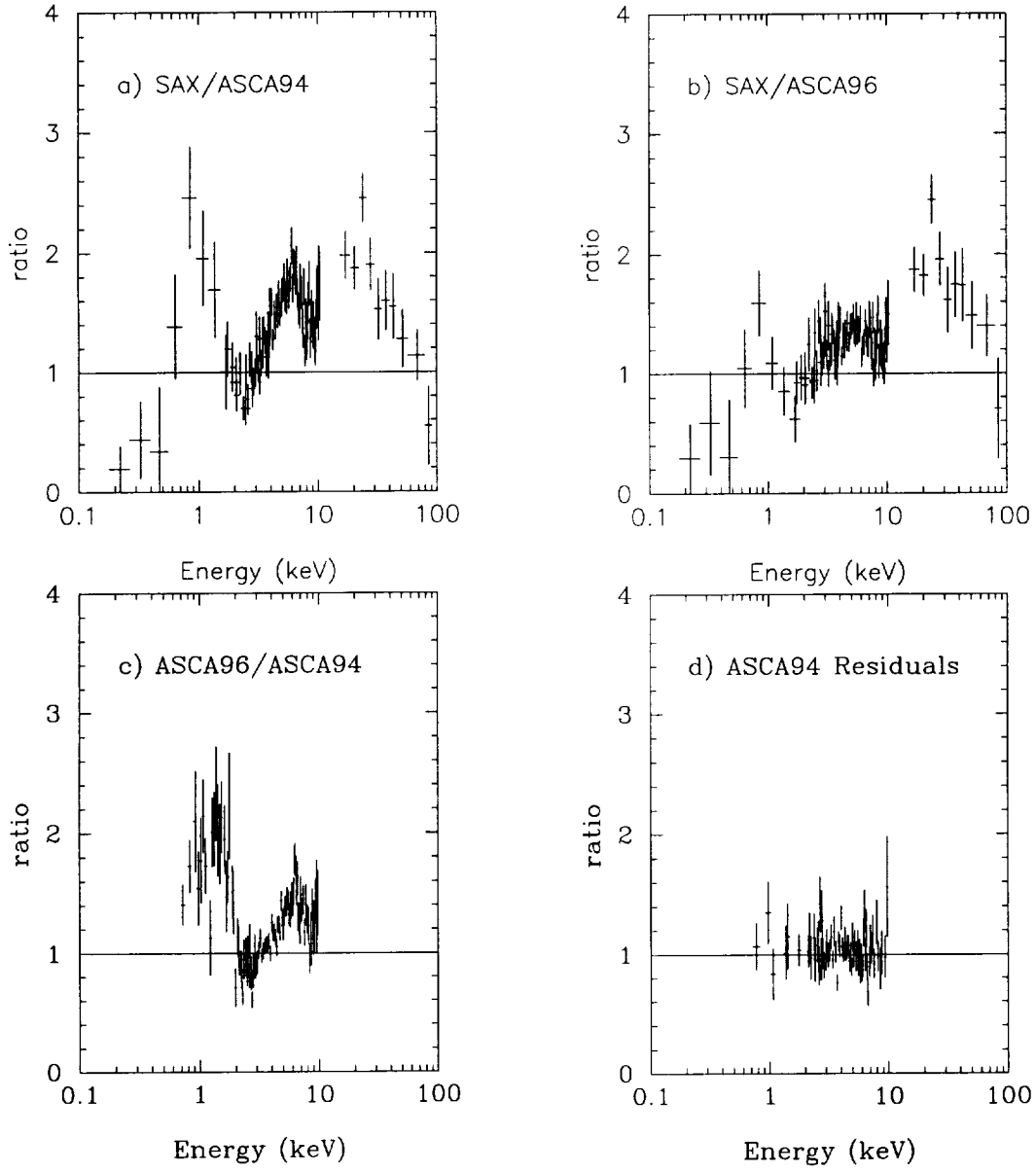


Fig. 6.— *a) The BeppoSAX data, compared to the model fitting the ASCA 1994 data; b) The BeppoSAX data compared to the second ASCA observation, from 1996; c) The ASCA data from 1996 compared to the model for the 1994 data; d) The ASCA residuals after a fit to the 1994 data*

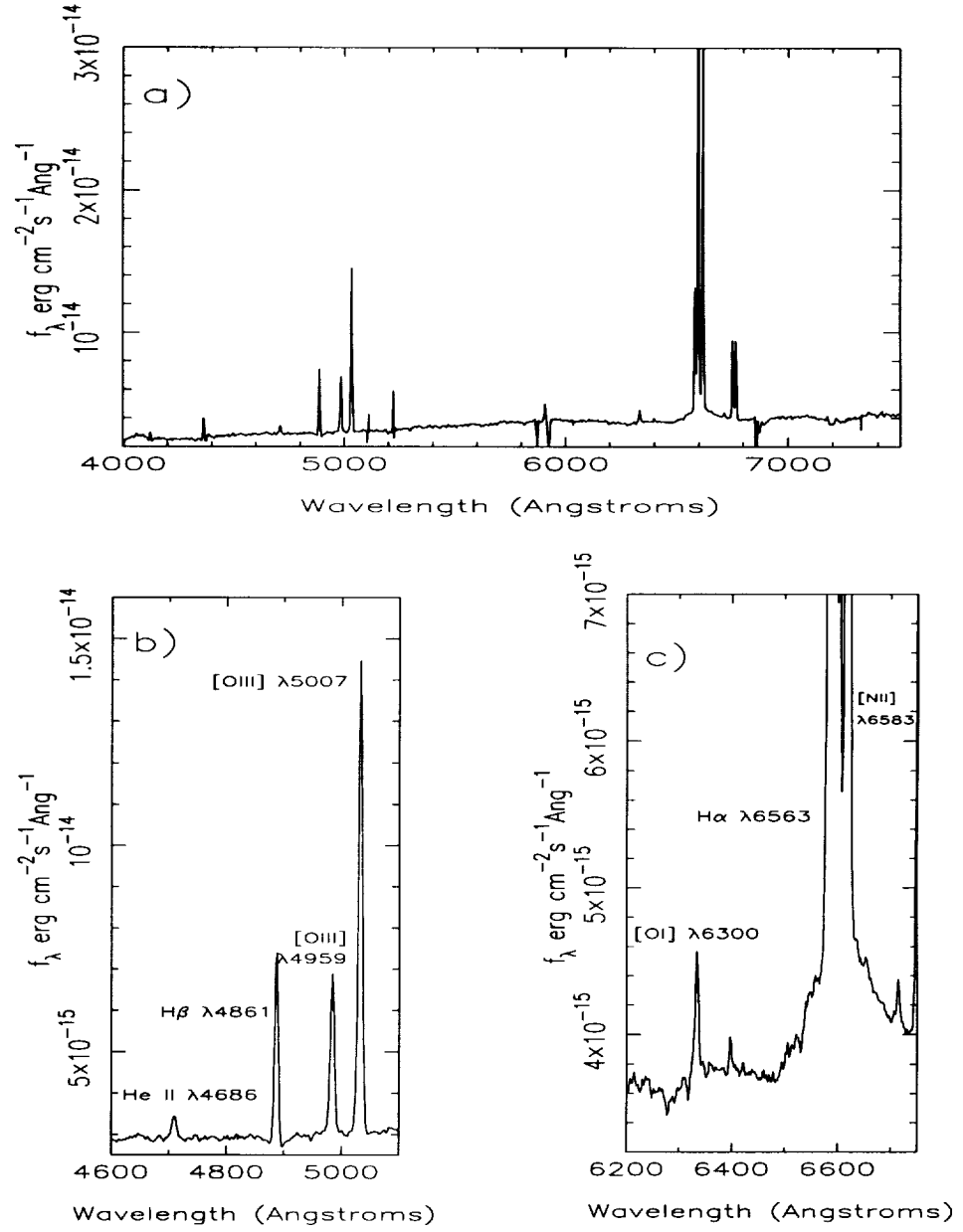


Fig. 7.— a) The optical spectrum of NGC 7582 ($z=0.0053$) taken at the CTIO 4m telescope; b) a close-up of the $H\beta$ region and c) a closeup of the $H\alpha$ region

REFERENCES

- Aretxaga, I., Joguet, B., Kunth, D., Melnick, J., Terlevich, R.J. 1999, *ApJ L*, in press (A99)
- Baldwin, J.A. & Stone, R.P.S., 1984, *MNRAS* 206, 241
- Boella, G., Butler, R.C., Perola, G.C., Piro, L., Scarsi, L., Bleeker, J.A.M. 1997a, *A&AS*, 122, 299
- Boella, G., et al. 1997b, *A&AS*, 122, 327
- Cappi, M., Mihara, T., Matsuoka, M., Brinkmann, W. Prieto, M.A., Palumbo, G.G.C. 1996, *ApJ* 456, 141
- Cappi, M., et al. 1999, *A&A* 344, 857
- Fiore, F., Guainazzi, M., Grandi, P. 1999, *A&A* submitted
- Frontera, F., Costa, E., Dal Fiume, D., Feroci, M., Nicastro, L., Orlandini, M., Palazzi, E., Zavattini, G. 1997, *SPIE* 3114, 206
- George, I.M., Fabian, A.C. 1991, *MNRAS* 249, 352
- George, I.M., Turner, T.J., Mushotzky, R.F., Nandra, K., Netzer, H. 1998, *ApJ* 503, 174
- Goodrich, R.W. 1989, *ApJ* 340, 190
- Goodrich, R.W. 1995, *ApJ* 440, 141
- Guainazzi, M., Matt, G., Antonelli, L.A., Fiore, F., Piro, L., Ueno, S. 1998, *MNRAS* 298, 824
- Halpern, J.P., Kay, L.E., Leighly, K. 1998, *IAU Circ* 7027
- Hayashi, I., Koyama, K., Awaki, H., Yamauchi, S., Ueno, S. 1996, *PASJ* 48, 219
- Heisler, C.A., Lumsden, S.L., Bailey, J.A. 1997, *Nature* 385, 700
- Johnson, W.N., Zdziarski, A.A., Madejski, G.M., Paciesas, W.S., Steinle, H., Lin, Ying-Chi, 1994, 4th Compton Symposium Proceedings, page 283. Ed. Charles D Dermer, Mark S. Strickman, James D Kurfess, AIP Woodbury, NY.
- Kaastra, J. S. 1992, , An X-Ray Spectral Code for Optically Thin Plasmas (Internal SRON-Leiden Report, updated version 2.0)
- Leahy, D.A., Creighton, J. 1993, *MNRAS* 263, 314
- Kriss, G.A. et al 1996, *ApJ* 467, 629
- Magdziarz, P., Zdziarski, A.A. 1995, *MNRAS* 273, 837
- Malaguti, G., et al. 1999, *A&A* 342, 41
- Matt, G. et al. 1997, *A&A* 325, L13

- Matt, G. et al. 1999, A&A 341, 39
- Oliva, E., Origlia, L., Kotilainen, J., Moorwood, A. 1995, A&A, 301, 55
- Parmar, A.N. et al. 1997, A&AS 122, 309
- Salvati, M., Bassani, L., Della Ceca, R., Maiolino, R., Matt, G., Zamorani, G. 1997 A&A 323, L1
- Schachter, J.F., Fiore, F., Elvis, M., Mathur, S., Wilson, A.S., Morse, J.A., Awaki, H., Iwasawa, K. 1998, ApJ503, L123
- Schlegel, E.M., 1990, MNRAS 244, 269
- Stark, A.A., Gammie, C.F., Wilson, R.W., Bally, J., Linke, R.A., Helies, C., Hurwitz, M. 1992, ApJS 79, 77
- Stone, R.P.S., Baldwin, J.A. 1983, MNRAS 204, 347
- Turner, T.J., George, I.M., Nandra, K., Mushotzky, R.F. 1997, ApJS 113, 23
- Vignali, C., Comastri, A., Stirpe, G.M., Cappi, M., Palumbo, G.G.C., Matsuoka, M., Malaguti, G., Bassani, L. 1998, A&A 333, 411
- Ward, M.J., Wilson, A.S., Penston, M.V., Elvis, M., Maccacaro, T., Tritton, K.P. 1978, ApJ, 223, 788
- Warwick, R.S., Sembay, S., Yaqoob, T., Makishima, K., Ohashi, T., Tashiro, M., Kohmura, Y. 1993, MNRAS 265, 412
- Xue, S-J., Otani, C., Mihara, T., Cappi, M., Matsuoka, M., 1998, PASJ 50, 519